University Library

MINERVA ACCESS

A gateway to Melbourne's research publications

Minerva Access is the Institutional Repository of The University of Melbourne

Author/s:
Palmer, LM;Clark, BA;Gründemann, J;Roth, A;Stuart, GJ;Häusser, M

Title:
Initiation of simple and complex spikes in cerebellar Purkinje cells

Date:
2010-05-01

Citation:
Palmer, L. M., Clark, B. A., Gründemann, J., Roth, A., Stuart, G. J. & Häusser, M. (2010). Initiation of simple and complex spikes in cerebellar Purkinje cells. Journal of Physiology, 588 (10), pp.1709-1717. https://doi.org/10.1113/jphysiol.2010.188300.

Persistent Link:
https://hdl.handle.net/11343/255933

License:
CC BY

J Physiol 588.10 (2010) pp 1709–1717

RAPID REPORT

Initiation of simple and complex spikes in cerebellar Purkinje cells

Lucy M. Palmer[1], Beverley A. Clark[2]*, Jan Gründemann[2], Arnd Roth[2], Greg J. Stuart[1] and Michael Häusser[2]

[1]*Department of Neuroscience, John Curtin School of Medical Research, Australian National University, Canberra, Australian Capital Territory 0200, Australia*

[2]*Wolfson Institute for Biomedical Research and Department of Neuroscience, Physiology, and Pharmacology, University College London, Gower Street, London WC1E 6BT, UK*

Cerebellar Purkinje cells produce two distinct forms of action potential output: simple and complex spikes. Simple spikes occur spontaneously or are driven by parallel fibre input, while complex spikes are activated by climbing fibre input. Previous studies indicate that both simple and complex spikes originate in the axon of Purkinje cells, but the precise location where they are initiated is unclear. Here we address where in the axon of cerebellar Purkinje cells simple and complex spikes are generated. Using extracellular recording and voltage-sensitive dye imaging in rat and mouse Purkinje cells, we show that both simple and complex spikes are generated in the proximal axon, ∼15–20 μm from the soma. Once initiated, simple and complex spikes propagate both down the axon and back into the soma. The speed of backpropagation into the soma was significantly faster for complex compared to simple spikes, presumably due to charging of the somatodendritic membrane capacitance during the climbing fibre synaptic conductance. In conclusion, we show using two independent methods that the final integration site of simple and complex spikes is in the proximal axon of cerebellar Purkinje cells, at a location corresponding to the distal end of the axon initial segment.

(Received 5 February 2010; accepted after revision 23 March 2010; first published online 31 March 2010)

Corresponding author G. Stuart: Department of Neuroscience, John Curtin School of Medical Research, Australian National University, Canberra, Australian Capital Territory 0200, Australia; M. Häusser: Wolfson Institute for Biomedical Research and Department of Neuroscience, Physiology and Pharmacology, University College London, Gower Street, London WC1E 6BT, UK. Email: greg.stuart@anu.edu.au and m.hausser@ucl.ac.uk

Introduction

Purkinje cells are the principal cells and the only output neurons of the cerebellar cortex, transmitting inhibitory signals to the deep cerebellar nuclei. The action potential output of Purkinje cells has been classified into two distinct types: simple spikes, which occur spontaneously (Häusser & Clark, 1997; Raman & Bean, 1997) and can exceed 100 Hz in response to excitation from parallel fibres (Eccles *et al.* 1967; Thach, 1967); and complex spikes, which are triggered by climbing fibre excitation and consist of a characteristic high-frequency burst (Eccles *et al.* 1967; Thach, 1967).

While both simple spikes and complex spikes are initiated in the axon of Purkinje cells (Stuart & Häusser, 1994; Clark *et al.* 2005; Khaliq & Raman, 2006; Davie *et al.* 2008), the precise location of spike generation is unknown. This information is critical, as the site of action potential initiation corresponds to the final site of synaptic integration and therefore the optimal location for modulation of neuronal output. While the axonal location of complex spike initiation has not previously been investigated, the axonal initiation site of simple spikes is unclear, with two studies using different methods to localize spike initiation arriving at different conclusions. An initial report using population data pooled from loose cell-attached recordings provided evidence consistent with an initiation site at the first node of Ranvier (Clark *et al.* 2005), whereas a subsequent study used sensitivity to local application of tetrodotoxin (TTX; a sodium channel blocker) and β-pompilidotoxin (which slows sodium channel inactivation) to conclude that initiation of simple spikes occurs instead in the axon initial segment (Khaliq & Raman, 2006). Both the initial segment and nodes of Ranvier of Purkinje cells contain high densities of sodium channels (Jenkins & Bennett, 2001; Komada & Soriano, 2002; Pan *et al.* 2006) making them both plausible

*L. M. Palmer and B. A. Clark contributed equally to this work.

© 2010 The Authors. Journal compilation © 2010 The Physiological Society

DOI: 10.1113/jphysiol.2010.188300

The Journal of Physiology

candidates as regions with a low threshold for action potential generation.

Here we aim to resolve this issue and address the question of where in Purkinje cell axons simple and complex spikes are generated using two complementary experimental techniques, together with compartmental modelling. First, we used multisite extracellular recordings along the Purkinje cell axon to provide a non-invasive readout of action potential initiation. Next, we used voltage-sensitive dye imaging to directly measure membrane potential changes simultaneously at multiple locations along Purkinje cell axons. These approaches both converge on the same conclusion: that initiation of simple and complex spikes normally occurs at the distal axon initial segment.

Methods

Slice preparation

Parasagittal slices (200–300 μm thick) from P18–28 rat (Sprague–Dawley and Wistar) and P18–25 mouse (L7-tau-GFP; Sekirnjak *et al.* 2003) cerebellum were made according to standard techniques (Stuart & Häusser, 1994). All procedures were approved by the UK Home Office and by the Animal Experimentation Ethics Committee of the Australian National University. Artificial cerebrospinal fluid (ACSF) for both slicing and electrophysiological recording contained (in mM): NaCl 125, KCl 2.5, $NaHCO_3$ 26, NaH_2PO_4 1.25, glucose 25, $MgCl_2$ 1, $CaCl_2$ 2. Voltage-sensitive dye experiments were carried out in a solution containing (in mM): NaCl 125, KCl 3, $NaHCO_3$ 25, NaH_2PO_4 1.25, glucose 25, $MgCl_2$ 1, $CaCl_2$ 2. These solutions were bubbled with 5% CO_2–95% O_2. Slices were initially incubated at 35°C for 30 min and subsequently maintained at room temperature (22°C). During recordings, slices were continuously superfused with ACSF and experiments were carried out at 34–35°C unless otherwise indicated.

Extracellular recording

Somatic whole-cell patch-clamp recordings were made from Purkinje cells under direct visual control (Stuart *et al.* 1993; Stuart & Häusser, 1994) using infrared differential interference contrast optics (Olympus BX50) and either Multiclamp 700A (Molecular Devices) or BVC-700 (Dagan) amplifiers. Whole-cell recording pipettes (3–10 MΩ prepared from filamented borosilicate glass) were filled with solution (280–285 mosmol kg^{-1}) containing (in mM): $KMeSO_4$ 130, KCl 7, Hepes 10, EGTA 0.05, Na_2ATP 2, MgATP 2, Na_2GTP 0.3, pH adjusted to 7.2 with KOH, to which 0.5% biocytin and 45–100 μM of the fluorescent dye AlexaFluor 488 or 594 were added. Neurons were visualized using a CCD camera as previously described (Monsivais *et al.* 2005) and control experiments confirmed that inclusion of AlexaFluor 488 or 594 and fluorescence visualization did not significantly affect action potential initiation or propagation (not shown). The presence of an intact (>200 μm) and accessible axon was confirmed before proceeding, and neurons were also filled with biocytin for subsequent morphological reconstruction. Data were low-pass filtered at 3–10 kHz before being sampled at 50–100 kHz using AxoGraph software (AxoGraph Scientific) using an ITC-16 or ITC-18 interface (Instrutech). A second patch pipette containing 150 mM NaCl was then used to record extracellular action potentials (eAPs) in current clamp mode from the soma and various locations along the axon during spontaneous firing. When axon collaterals were present within the first 200 μm, the collateral branch point was always one of the recording sites. Spontaneous somatic action potentials were detected and on-line spike-triggered averaging (typically 100–200 sweeps) was used to optimize the precise placement of the recording electrode in order to maximize the signal-to-noise ratio for recording extracellular spikes at each recording site. *Post hoc* biocytin staining allowed verification of axonal recording distances from the soma. Some recordings were also made from the same sites in loose cell-attached voltage-clamp mode using previously described methods (Clark *et al.* 2005). Complex spikes were evoked by climbing fibre stimulation using a patch electrode, filled with ACSF, placed in the granule cell layer (Davie *et al.* 2008).

Voltage sensitive dye imaging

Somatic whole-cell patch-clamp recordings were made from Purkinje cells as described above using pipettes tip-filled with internal solution containing (in mM): potassium gluconate 135, NaCl 7, $MgCl_2$ 2, Hepes 10, Na_2ATP 2, Na_2GTP 0.3 (pH adjusted to 7.2 with KOH), and back-filled with internal solution containing 1–3 mg ml^{-1} of the voltage-sensitive dye JPW3028 (the di-methyl analogue of JPW1114 (Antic & Zecevic, 1995), synthesized and provided by J. P. Wuskell and L. M. Loew, University of Connecticut, Farmington, CT, USA). Whole-cell recordings were maintained for 45–60 min to allow diffusion of dye into the neuron before the patch pipette was removed. The dye-filled neuron was left undisturbed for up to 2 h before being repatched (Antic *et al.* 1999). Voltage-sensitive dye fluorescence changes were detected with a back-illuminated cooled CCD camera (Red Shirt Imaging, Fairfield, CT, USA) operating at 10 kHz (80 × 12 pixel resolution) using Neuroplex software (Red Shirt Imaging). Excitation was achieved using a 150 W xenon (Opti Quip, Highland Mills, NY, USA) or 100 W halogen (Olympus) lamp gated by a shutter (Uniblitz, Rochester, NY, USA). Voltage-sensitive dye

© 2010 The Authors. Journal compilation © 2010 The Physiological Society

excitation and emission were obtained using appropriate filters (excitation 520 ± 45 nm, dichroic 570 nm, emission >610 nm). Purkinje cell axonal and dendritic morphology could readily be visualized because of the high resting fluorescence of voltage-sensitive dyes. To maximize the signal-to-noise ratio of the optical signal in the axon we used regions of interest (ROIs) of 3 pixels length (∼10 μm) and 2 pixels width (∼6 μm), and typically averaged 100 individually aligned responses. Responses to both simple spikes (spontaneous or evoked by steady-state somatic current injection) and complex spikes were recorded at the soma and simultaneously at multiple ROIs in the axon. Experiments were discontinued if the amplitude of somatic action potentials decreased by more than 5% during the recording. For display purposes only, fluorescence signals were low-pass filtered at 1 kHz.

Analysis

Data were analysed in Igor Pro (Wavemetrics, Lake Oswego, OR, USA), together with NeuroMatic software (http://www.neuromatic.thinkrandom.com/), or using AxoGraph (AxoGraph Scientific). Averages of axonal and somatic extracellularly recorded spikes were generated by alignment to the peak of the first derivative of the somatic action potential recorded simultaneously in whole-cell mode. Axosomatic delays were calculated by locating the time when the extracellular spike at each axonal location reached 10% of its maximum height (10% rise point) and subtracting the time of the 10% rise point of the somatic extracellular spike. The 10% rise point was chosen because it is dominated by the onset of the local sodium current in the axon initial segment and the first node of Ranvier and is not contaminated by other ionic currents and therefore enables reliable detection of the locus of spike initiation. This is illustrated using simulations shown in the online Supplemental Material (Figs S1 and S2). For voltage-sensitive dye signals, individual trials were also aligned using the action potential recorded via the somatic recording pipette to remove trial-to-trial temporal jitter. Fluorescence changes were not filtered, and the amplitude of the optical signal was expressed as the percentage change in light intensity divided by the resting light intensity ($\Delta F/F$). The delay of axonal fluorescence signals relative to those at the soma was measured at half amplitude after fitting a linear regression to the rising phase of the fluorescence change (Palmer & Stuart, 2006). This criterion was chosen to minimize the influence of noise on the measurement of the axosomatic delay, but qualitatively similar results were obtained when axosomatic delay for voltage-sensitive dye signals was based on the time to reach 10% of peak amplitude. Because the membrane potential waveform during the action potential in the axon differs from that of the soma (Stuart & Häusser, 1994; Geiger & Jonas, 2000; Kole *et al.* 2007; Schmidt-Hieber *et al.* 2008), and because the different recording techniques measure different quantities derived from the action potential waveform, it is not possible to directly compare axosomatic delays measured using the different techniques. For the moving averages shown in Fig. 3, data points were first sorted according to distance, averaged if several data points were measured at the same distance, and padded with points representing the soma (0 μm distance, 0 μs delay). In Fig. 4, complex spikes preceded by a simple spike within ∼1.5 ms were excluded from analysis.

Results

Determination of the site of simple spike initiation using extracellular recording

Simultaneous somatic whole-cell recordings and extracellular recordings from multiple locations along the axon (Fig. 1*A*) were made from rat Purkinje cells visualized in sagittal cerebellar slices. Figure 1*B* shows extracellular action potentials (eAPs) recorded from a Purkinje cell soma and various axonal locations. Average spike-triggered voltage transients recorded at each site are displayed in order of distance from the soma, aligned to the peak dV/dt of the somatic action potential. Axosomatic delays were calculated from the 10% rise point of each averaged axonal eAP relative to that of the eAP at the soma. Since extracellular voltage signals may be influenced by currents arising at distant locations we used simulations of eAP generation in two compartmental models to verify that our recordings were dominated by local current sources in the initial segment and first node and that multisite extracellular recordings can distinguish between the initiation of spikes at these two locations (see Supplemental Figs S1 and S2). Briefly, we used a previously published model (Clark *et al.* 2005), in which action potentials were initiated at the first node of Ranvier, and modified it by adjusting ion channel densities so that action potentials were instead initiated in the axon initial segment. These two versions of the model were then used to simulate eAPs and show that they can be used to reliably detect the location of the initiation site.

Figure 1*C* shows the relationship between the axosomatic delay of axonal eAPs and the corresponding distance of the axonal recording site from the soma for six different Purkinje cells for which the axon was sampled at five or more locations within the first 200 μm. Arrows indicate the axonal location for each cell where the axosomatic delay was longest, i.e. the location of maximal advance of the axonal *vs.* the somatic eAP. The axonal site with the longest axosomatic delay is by definition the site of simple spike generation. In the cell shown in Fig. 1*A*, this occurred at the axonal recording site closest to the soma, corresponding to the axon initial segment, which

© 2010 The Authors. Journal compilation © 2010 The Physiological Society

in rat cerebellar Purkinje cells is approximately 20 μm long (Somogyi & Hamori, 1976; Clark *et al.* 2005). At the location with the longest axosomatic delay, on average, the onset of the simple spike in the axon occurred 206 $\pm$ 22 μs before the somatic action potential, at a distance from the axon hillock of 22 $\pm$ 8 μm (n = 11). Although in one cell the axon spike was most advanced at an axonal location 95 μm from the soma, in the majority of cells (10/11) the longest axosomatic delay was found within the first 25 μm, at locations corresponding to the axon initial segment, suggesting that simple spike initiation usually occurs within this zone. Similar results were obtained in recordings made from mouse Purkinje cells, where the average axonal distance with the longest axosomatic delays was at 20 $\pm$ 4 μm from the soma (n = 7; Supplemental Fig. S3).

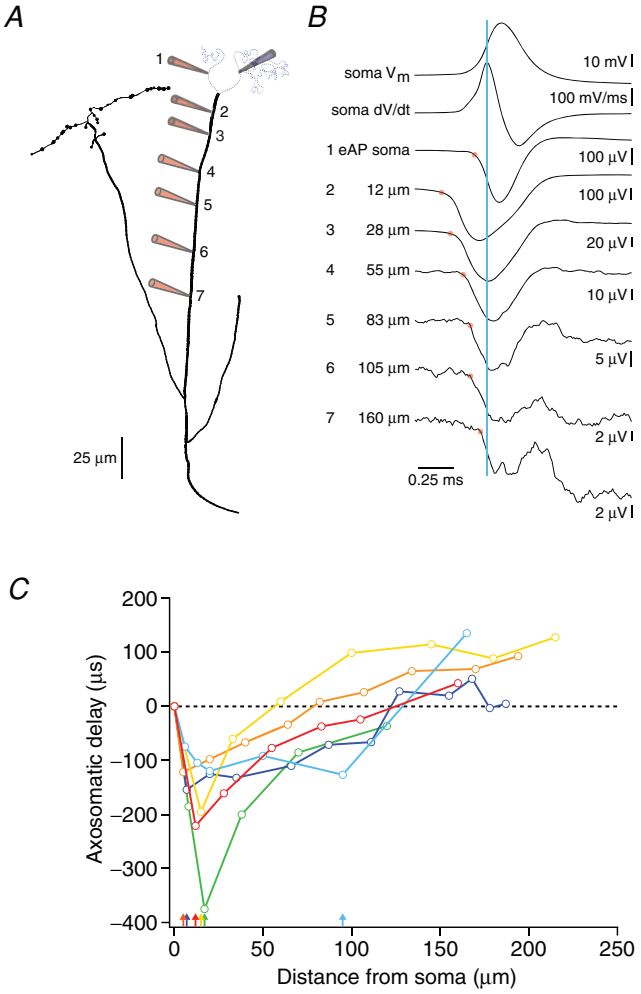

Figure 1. Extracellular action potential recording of simple spike initiation
A, Neurolucida reconstruction of the soma and axon of a Purkinje cell indicating the location of extracellular recording sites (red pipettes). *B*, whole-cell voltage recording of spontaneous simple spikes (top trace) and extracellular recording of simple spikes at the soma and the indicated axon locations (same cell as in *A*). Data aligned to the peak of the somatic d*V*/d*t* (vertical line). Red circles indicate the time when the eAP reaches 10% of its maximum amplitude. *C*, axosomatic delays for data shown in *B* (red) and for 5 other cells (each indicated by a separate colour) plotted with respect to axonal distance of the recording sites. Coloured arrows mark the location of the minima for each cell.

Determination of the site of simple spike initiation with voltage-sensitive dyes

We next used an orthogonal approach for localizing the initiation site in the axon: voltage-sensitive dye imaging (Antic & Zecevic, 1995; Palmer & Stuart, 2006). The advantage of this method is that it allows the simultaneous recording of voltage at multiple locations. Rat Purkinje cells were filled with voltage-sensitive dye (Fig. 2*A*) and fluorescence changes during simple spikes were recorded simultaneously at the soma and different locations along the axon (Fig. 2*B*). The axosomatic delay of fluorescence signals was defined as the time difference between the axonal and somatic fluorescence $\Delta F/F$ measured at half-amplitude after fitting a linear regression to the rising phase of both signals. The axonal site with the longest axosomatic delay ranged from 5 to 25 μm from the axon hillock (coloured arrows in Fig. 2*C*). On average, the longest delay was 144 $\pm$ 47 μs (n = 4) at a distance from the axon hillock of 15 $\pm$ 4 μm (n = 4). Similar results were obtained during recordings at room temperature, where the longest axosomatic delay was 199 $\pm$ 16 μs at a location 17 $\pm$ 3 μm from the axon hillock (n = 9; data not shown).

Purkinje cell simple spikes are normally initiated in the axon initial segment

A comparison of the distance dependence of axosomatic delays measured using three different techniques (extracellular recording, voltage-sensitive dye imaging and cell-attached capacitive current recording) is shown in Fig. 3. Cell-attached recordings were compiled from previously published data (Clark *et al.* 2005) together with additional new data points. For each method, raw pooled data are shown in Fig. 3*A*. By smoothing this data either by binning (Fig. 3*B*) or by using a 10-point moving average (Fig. 3*C*) the location of distinct minima (i.e. points of longest delay; arrows, Fig. 3*C*) becomes apparent. Unlike a bilinear fit (Clark *et al.* 2005; Meeks *et al.* 2005), the 10-point moving average does not impose a specific hypothesis regarding the shape of the distance–delay relationship on the data. Both the extracellular (left column of Fig. 3*C*) and the voltage-sensitive dye data (middle column of Fig. 3*C*) showed single minima at very similar locations of 14 and 13 μm, respectively, based on the 10-point moving average (note that these values are slightly different from those reported above due to the different averaging procedure, and because the pooled

© 2010 The Authors. Journal compilation © 2010 The Physiological Society

data used here include data points from additional cells in which fewer than five axonal locations were sampled). In contrast, the 10-point moving average of the cell-attached data showed two distinct minima (at 29 μm and at 78 μm), with the global minimum being more distant from the soma.

Our experiments and simulations indicate that the most likely explanation for the discrepancy between the extracellular and voltage-sensitive dye data on one hand and the cell-attached data on the other is the difficulty in discriminating the contribution of capacitive and ionic (sodium and/or potassium) current in cell-attached recordings (Colbert & Johnston, 1996; Perkins, 2006). During action potential propagation, the capacitive component usually dominates cell-attached currents recorded from myelinated sections of the axon. However, cell-attached recordings from non-myelinated axonal regions such as the axon initial segment, which contain a high density of voltage-activated channels, frequently contain a contribution of ionic (in particular sodium) current. This can distort the cell-attached current waveform, and therefore influence the estimated timing of the axonal action potential. In the most extreme cases, positive initial deflections in these recordings (see Supplemental Fig. S4) indicate that the recorded current waveform is dominated by ionic (presumably sodium) current. Although these more extreme cases were not used for analysis, they suggest that a significant fraction of cell-attached recordings from the initial segment may be contaminated by ionic current. This could adversely affect the estimate of the initiation site when compiling data across multiple cell-attached recordings from multiple cells using a simple V-plot to fit the data. Interestingly, the moving average revealed two minima in the cell-attached data – one closest to the initial segment, and the second closer to the first node. This is consistent with the small minority of cells in eAP and voltage-sensitive dye recordings (2 in 23; $<10\%$) exhibiting two discrete minima in axosomatic delay *versus* distance plots, suggesting either simultaneous initiation at the initial segment and node, first node initiation or switching of initiation between these two sites. We conclude that multisite extracellular recording and voltage-sensitive dye imaging represent more accurate methods for determining the location of the initiation site in the axon.

The site of initiation of the complex spike

The site of action potential initiation during complex spikes is unknown. We addressed this issue using voltage-sensitive dye imaging during complex spikes evoked by climbing fibre input in rat Purkinje cells. Figure 4 shows voltage-sensitive dye responses recorded at the soma and different axonal locations in a Purkinje cell during a complex spike. The first spike in the complex spike had the longest axosomatic delay at approximately the same axonal site as the simple spike (Fig. 4*C*), both at physiological temperature (open circles; 18 ± 3 μm from the axon hillock; $n = 3$) and room temperature (filled circles; 15 ± 4 μm from the axon hillock; $n = 4$; $P > 0.05$). The location in the Purkinje cell axon where simple and complex spikes were initiated (16 ± 3 μm when combining data from room and physiological

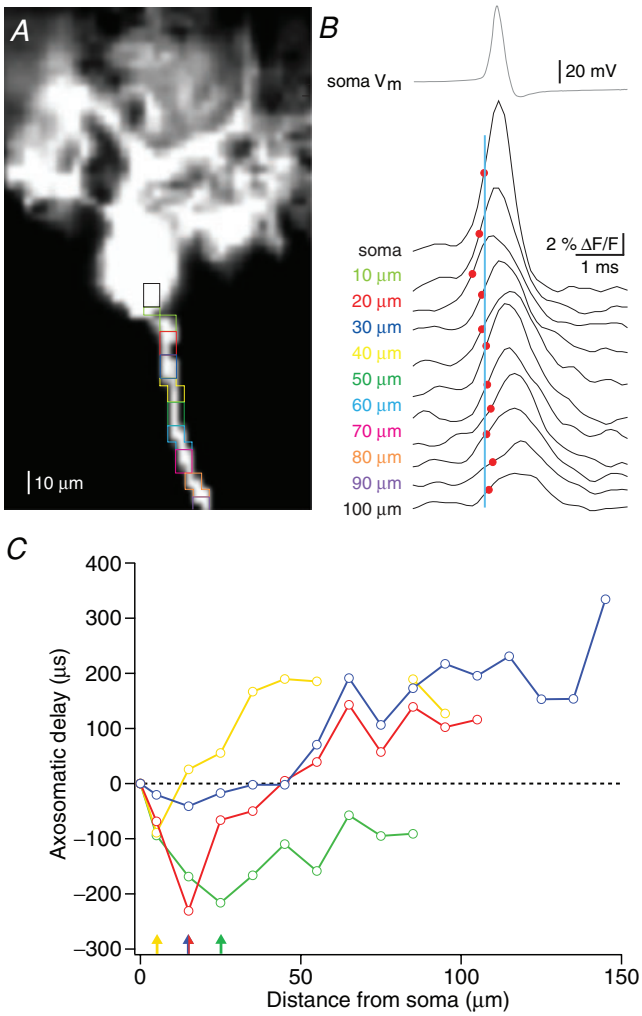

Figure 2. Voltage-sensitive dye imaging of simple spike initiation
A, image of a cerebellar Purkinje cell filled with voltage-sensitive dye. *B*, somatic whole-cell recording of a spontaneous simple spike (top, grey) in the cell shown in *A* together with corresponding axonal fluorescence responses (black) at the indicated locations detected using voltage-sensitive dye imaging. Red circles indicate the time when the response reaches 50% of its maximum amplitude. The fluorescence response in the proximal axon (20 μm from the hillock) precedes that in the soma and all other axonal locations. Coloured labels correspond to the coloured boxes in *A*, indicating the regions of interest. *C*, axosomatic delays for data shown in *B* (red) and 3 other cells (each indicated by a separate colour) plotted with respect to axonal distance of the recording sites. Coloured arrows mark the location of the minima for each cell.

© 2010 The Authors. Journal compilation © 2010 The Physiological Society

temperature) was not significantly different ($P > 0.05$). This indicates that, like simple spikes, complex spikes are initiated in the proximal axon, at a region corresponding to the distal axon initial segment.

Interestingly, at the initiation site, the axonal waveform of the first spike in the complex spike preceded that at the soma by $42 \pm 16\ \mu$s ($n = 7$; combined data from room and physiological temperature). This is significantly less than the time taken for propagation of simple spikes from their site of initiation to the soma (~150–200 μs; $P < 0.05$; combined data from room and physiological temperature), indicating that the propagation speed of the first spike in the complex spike to the soma is significantly faster than during simple spikes.

Discussion

We have used two different approaches – multisite extracellular recording and voltage-sensitive dye imaging – to determine the site of initiation of action potentials in cerebellar Purkinje neurons. Previous work indicated that both simple and complex spikes are generated in the axon of Purkinje cells (Stuart & Häusser, 1994; Clark *et al.* 2005; Khaliq & Raman, 2006; Davie *et al.* 2008), but the precise location of the initiation site has not been directly determined. Here we show, using direct methods, that both simple and complex spikes are normally generated in the proximal axon of Purkinje cells, approximately ~15–20 μm from the soma. Our findings indicate that the final site of integration of synaptic input in Purkinje cells is in the proximal axon, at the distal end of the axon initial segment. This is consistent with recent findings in neocortical pyramidal neurons (Palmer & Stuart, 2006; Kole *et al.* 2007; Shu *et al.* 2007), suggesting that this may be a general feature of synaptic integration in mammalian central neurons.

The initiation site of simple and complex spikes is normally in the axon initial segment

We have used two independent methods to determine the initiation site in cerebellar Purkinje cells in slices:

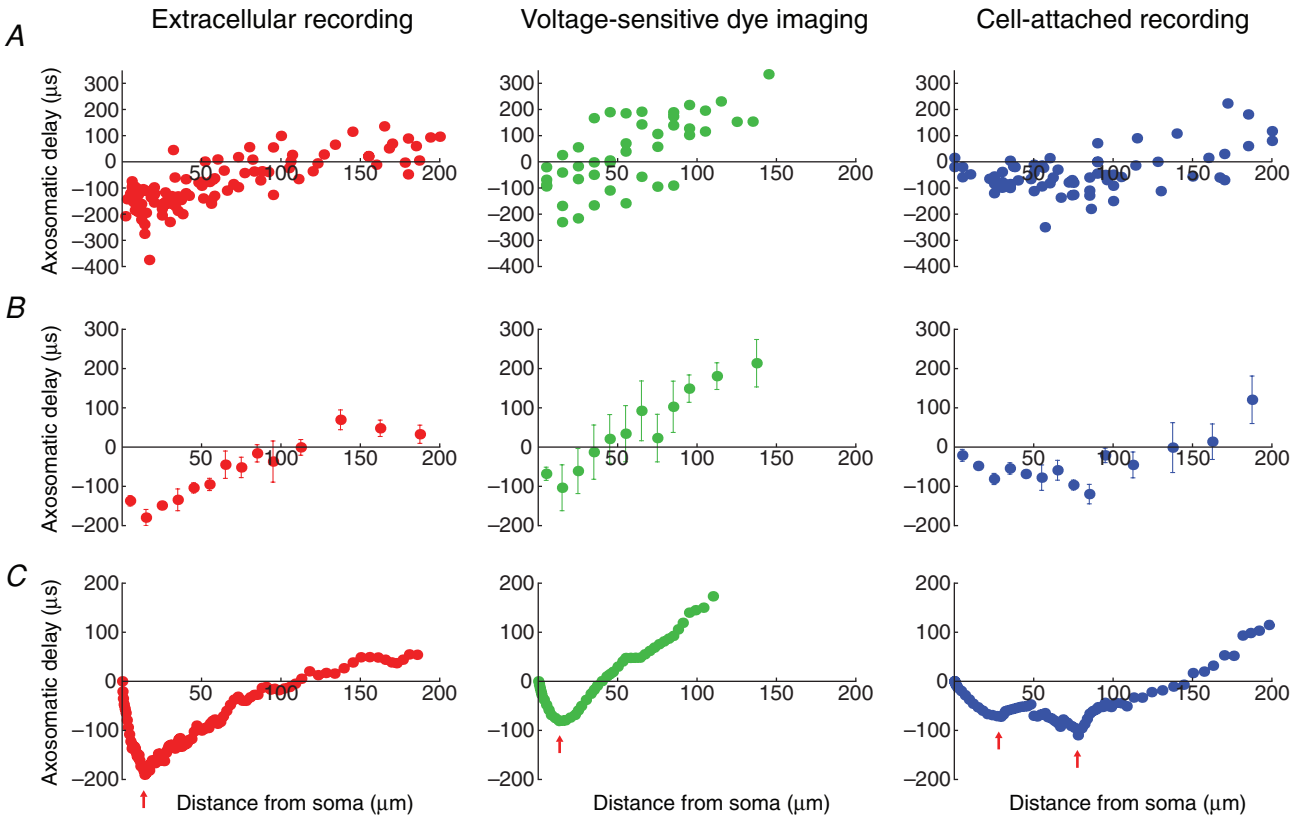

Figure 3. Comparison of simple spike data recorded using three different methods
A, synopsis of axosomatic delays measured using extracellular recording (left), voltage-sensitive dye imaging (middle) and cell-attached recording (right). Each data point corresponds to a single axonal location. Data points are from 17, 4 and 80 cells, respectively. *B*, axosomatic delays calculated by binning the data in *A* according to distance. Bin width was 10 μm for distances up to 100 μm and 25 μm for larger distances. Error bars indicate S.E.M. *C*, 10-point moving average of the data in *A*. Red arrows mark the location of the minima of the axosomatic delay in each population.

© 2010 The Authors. Journal compilation © 2010 The Physiological Society

multisite extracellular recordings and voltage-sensitive dye imaging. Results using both methods converge on the same conclusion: that the site of action potential initiation in the Purkinje cell axon is normally ~15–20 μm from the soma. Since the length of the axon initial segment in rat and mouse Purkinje cells is approximately 20 μm (Somogyi & Hamori, 1976; Clark *et al.* 2005), this indicates that the initiation site is at the end of the axon initial segment. That both simple and complex spikes exhibit the same initiation site indicates that this location is normally robust under a variety of different stimulation paradigms. Not all neurons exhibited spike initiation solely in the initial segment, however, as we observed two cells (out of 23) where initiation occurred either at the first node or simultaneously at the first node and initial segment. The reasons for this cell-to-cell variability may be structural (e.g. due to geometric factors such as axon diameter or axonal branching; or location of myelination) or due to cell-to-cell differences in the distribution or properties of voltage-gated channels in the axon. Overall the results validate the conclusions of Khaliq & Raman (2006) who used pharmacological approaches to identify the axon initial segment as the initiation site for simple spikes, and are inconsistent with the conclusion, based on data pooled from cell-attached recordings, that action potentials are usually initiated at the first node of Ranvier (Clark *et al.* 2005). The most likely explanation for the discrepancy with the earlier study by Clark *et al.* (2005) is that cell-attached recordings from the axon initial segment can exhibit overlap of capacitive and ionic current waveforms, leading to an unreliable assignment of the site of action potential initiation when fitting a simple V-plot to the population data across multiple cells. Interestingly, while both simple and complex spikes are initiated at the same location, the first spike of the complex spike backpropagates into the soma approximately three times faster than the simple spike. This is likely to be due to pre-charging of the membrane capacitance of the soma and dendrites by the climbing fibre synaptic conductance, which mitigates the capacitive load of the soma and dendrites (Bekkers & Häusser, 2007) and enhances propagation speed.

Action potential initiation and comparisons with previous studies

Our result that both the simple spike and the first component of the complex spike are initiated in the proximal axon supports recent findings in other neuronal cell types showing that the axon initial segment is the site of action potential initiation. Early work in spinal motoneurons (Coombs *et al.* 1957) showed that the somatic action potential has two components: a smaller initial segment (IS) spike and a larger somato-dendritic (SD) spike. The IS spike is always preceded by the SD spike independent of whether action potentials are evoked by orthodromic or antidromic stimulation, leading to the hypothesis that action potentials are initiated in the proximal axon. While indirect methods indicated a more distal initiation site (Colbert & Johnston, 1996), subsequent studies have used direct recordings from the axon, or voltage-sensitive dye imaging, to identify the precise

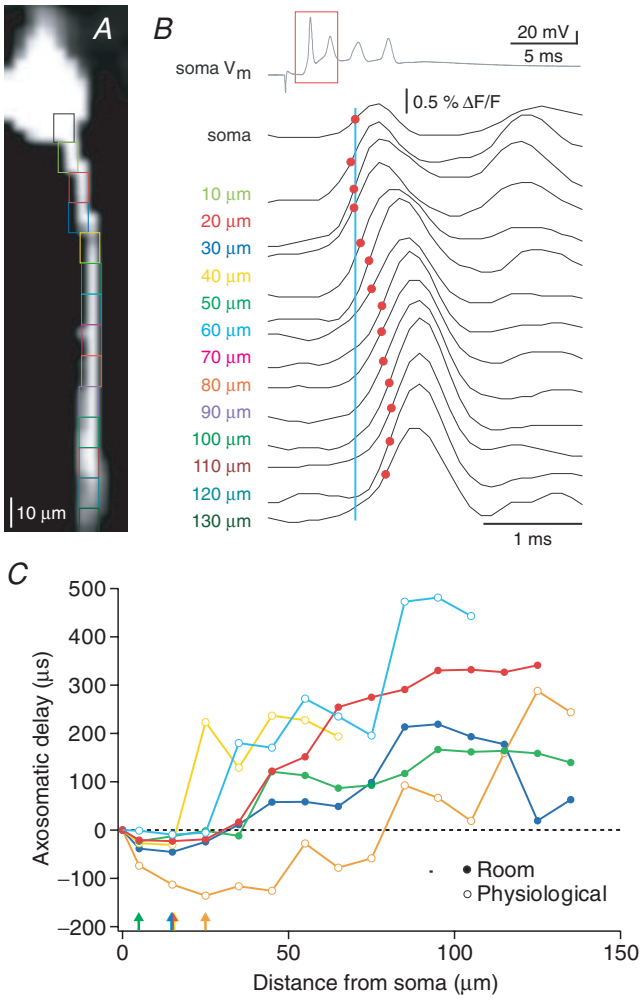

Figure 4. Voltage-sensitive dye imaging of complex spike initiation
A, image of a cerebellar Purkinje cell filled with voltage-sensitive dye. *B*, somatic whole-cell recording of a complex spike (top, grey) in the Purkinje cell shown in *A* together with corresponding axonal fluorescence responses (black) at the indicated locations detected using voltage-sensitive dye imaging. Red circles indicate the time when the first spike in the complex spike fluorescence response reaches 50% of its maximum amplitude. The fluorescence trace in the proximal axon (red; 10 μm from the hillock) slightly precedes the soma and all other axonal locations. Coloured labels correspond to the coloured boxes in *A*, indicating the location of regions of interest. *C*, axosomatic delays for the first spike in the complex spike for 6 Purkinje cells (each indicated by a separate colour; the red trace is the data shown in *B*) recorded at physiological (open circles) and room temperature (filled circles). Coloured arrows mark the location of the minima for each cell.

© 2010 The Authors. Journal compilation © 2010 The Physiological Society

location of the initiation site in the axon. These studies have concluded that the initiation site is in the initial segment in layer 5 pyramidal cells in rats (Palmer & Stuart, 2006) and ferrets (Shu *et al.* 2007), and that the proximal axon is the initiation site in CA3 pyramidal neurons (Meeks & Mennerick, 2007) and dentate gyrus granule cells (Kress *et al.* 2008; Schmidt-Hieber *et al.* 2008).

The conservation of the action potential initiation site across different neuron types is somewhat surprising considering their diverse morphologies. Purkinje cells have an extensive dendritic tree that lacks voltage-activated sodium channels (Stuart & Häusser, 1994) and is likely to exert a significantly greater electrical load on the soma than in layer 5 pyramidal neurons (Bekkers & Häusser, 2007). Despite these obvious morphological and physiological differences, the action potential is normally initiated in the distal end of the initial segment in both myelinated and non-myelinated axons in all cell types and species so far investigated, indicating that this appears to be a general principle for synaptic integration in mammalian central neurons.

Functional implications

What are the functional implications of the initiation site being at the end of the initial segment? The unitary location of the initiation site for both simple and complex spikes provides a single target for modulation of spike initiation (Stuart *et al.* 1997). This is consistent with the known pattern of innervation of inhibitory synaptic input to Purkinje cells, which is concentrated in the initial segment via the dense innervation by basket cell axons, forming the characteristic pinceau (Eccles *et al.* 1967). Initiation of simple and complex spikes at the distal initial segment at a site close to the soma would also be expected to maximize synaptic efficacy, and to ensure maximal precision in the timing of action potentials triggered by transient synaptic inputs. Together, these considerations suggest that initiation of both simple and complex spikes at the distal axon initial segment may have important implications for normal cerebellar function.

References

Antic S & Zecevic D (1995). Optical signals from neurons with internally applied voltage-sensitive dyes. *J Neurosci* **15**, 1392–1405.

Antic S, Major G & Zecevic D (1999). Fast optical recordings of membrane potential changes from dendrites of pyramidal neurons. *J Neurophysiol* **82**, 1615–1621.

Bekkers JM & Häusser M (2007). Targeted dendrotomy reveals active and passive contributions of the dendritic tree to synaptic integration and neuronal output. *Proc Natl Acad Sci U S A* **104**, 11447–11452.

Clark BA, Monsivais P, Branco T, London M & Häusser M (2005). The site of action potential initiation in cerebellar Purkinje neurons. *Nat Neurosci* **8** 137–139.

Colbert CM & Johnston D (1996). Axonal action-potential initiation and Na^+ channel densities in the soma and axon initial segment of subicular pyramidal neurons. *J Neurosci* **16**, 6676–6686.

Coombs JS, Curtis DR & Eccles JC (1957). The interpretation of spike potentials of motoneurones. *J Physiol* **139**, 198–231.

Davie JT, Clark BA & Häusser M (2008). The origin of the complex spike in cerebellar Purkinje cells. *J Neurosci* **28**, 7599–7609.

Eccles JC, Ito M & Szentagothai J (1967). *The Cerebellum as a Neuronal Machine*. Springer, Berlin.

Geiger JRP & Jonas P (2000). Dynamic control of presynaptic Ca^{2+} inflow by fast-inactivating K^+ channels in hippocampal mossy fibre boutons. *Neuron* **28**, 927–939.

Häusser M & Clark BA (1997). Tonic synaptic inhibition modulates neuronal output pattern and spatiotemporal synaptic integration. *Neuron* **19**, 665–678.

Jenkins SM & Bennett V (2001). Ankyrin-G coordinates assembly of the spectrin-based membrane skeleton, voltage-gated sodium channels, and L1 CAMs at Purkinje neuron initial segments. *J Cell Biol* **155**, 739–746.

Khaliq ZM & Raman IM (2006). Relative contributions of axonal and somatic Na channels to action potential initiation in cerebellar Purkinje neurons. *J Neurosci* **26**, 1935–1944.

Kole MHP, Letzkus JJ & Stuart GJ (2007). Axon initial segment Kv1 channels control axonal action potential waveform and synaptic efficacy. *Neuron* **55**, 633–647.

Komada M & Soriano P (2002). βIV-spectrin regulates sodium channel clustering through ankyrin-G at axon initial segments and nodes of Ranvier. *J Cell Biol* **156**, 337–348.

Kress GJ, Dowling MJ, Meeks JP & Mennerick S (2008). High threshold, proximal initiation, and slow conduction velocity of action potentials in dentate granule neuron mossy fibres. *J Neurophysiol* **100**, 281–291.

Meeks JP, Jiang X & Mennerick S (2005). Action potential fidelity during normal and epileptiform activity in paired soma-axon recordings from rat hippocampus. *J Physiol* **566**, 425–441.

Meeks JP & Mennerick S (2007). Action potential initiation and propagation in CA3 pyramidal axons. *J Neurophysiol* **97**, 3460–3472.

Monsivais P, Clark BA, Roth A & Häusser M (2005). Determinants of action potential propagation in cerebellar Purkinje cell axons. *J Neurosci* **25**, 464–472.

Palmer LM & Stuart GJ (2006). Site of action potential initiation in layer 5 pyramidal neurons. *J Neurosci* **26**, 1854–1863.

Pan Z, Kao T, Horvath Z, Lemos J, Sul J-Y, Cranstoun SD, Bennett V, Scherer SS & Cooper EC (2006). A common ankyrin-G-based mechanism retains KCNQ and Na_v channels at electrically active domains of the axon. *J Neurosci* **26**, 2599–2613.

Perkins KL (2006). Cell-attached voltage-clamp and current-clamp recording and stimulation techniques in brain slices. *J Neurosci Methods* **154**, 1–18.

© 2010 The Authors. Journal compilation © 2010 The Physiological Society

Raman IM & Bean BP (1997). Resurgent sodium current and action potential formation in dissociated cerebellar Purkinje neurons. *J Neurosci* **12**, 4517–4526.

Schmidt-Hieber C, Jonas P & Bischofberger J (2008). Action potential initiation and propagation in hippocampal mossy fibre axons. *J Physiol* **586**, 1849–1857.

Sekirnjak C, Vissel B, Bollinger J, Faulstich M & du Lac S (2003). Purkinje cell synapses target physiologically unique brainstem neurons. *J Neurosci* **23**, 6392–6398.

Shu Y, Duque A, Yu Y, Haider B & McCormick DA (2007). Properties of action-potential initiation in neocortical pyramidal cells: evidence from whole cell axon recordings. *J Neurophysiol* **97**, 746–760.

Somogyi P & Hamori J (1976). A quantitative electron microscopic study of the Purkinje cell axon initial segment. *Neuroscience* **1**, 361–365.

Stuart GJ, Dodt HU & Sakmann B (1993). Patch-clamp recordings from the soma and dendrites of neurons in brain slices using infrared video microscopy. *Pflügers Arch* **423**, 511–518.

Stuart G & Häusser M (1994). Initiation and spread of sodium action potentials in cerebellar Purkinje cells. *Neuron* **13**, 703–712.

Stuart G, Spruston N, Sakmann B & Häusser M (1997). Action potential initiation and backpropagation in neurons of the mammalian CNS. *Trends Neurosci* **20**, 125–131.

Thach WT Jr (1967). Somatosensory receptive fields of single units in cat cerebellar cortex. *J Neurophysiol* **30**, 675–696.

Author's present address

L.M. Palmer: Department of Physiology, University of Bern, Bühlplatz 5, 3012 Bern, Switzerland.

Author contributions

All authors designed the study and wrote the paper. L.M.P. performed and analysed the voltage imaging experiments at the John Curtin School of Medical Research, Canberra, Australia. B.A.C & J.G. performed and analysed the electrophysiological recordings and J.G. & A.R. carried out the modelling at the WIBR, UCL, London, UK.

Acknowledgements

We are grateful to Mickey London, Christoph Schmidt-Hieber, Arne Nagengast, Julian Jack and Jenny Davie for helpful discussions and for their comments on the manuscript. This work was supported by grants from the National Health and Medical Research Council of Australia, the Wellcome Trust, European Commission, EPSRC and the Gatsby Foundation.

© 2010 The Authors. Journal compilation © 2010 The Physiological Society